Estimation of Double Star Parameters by Speckle Observations Using a Webcam

Roberto Maria Caloi

Unione Biellese Astrofili - Gruppo Astrofili Eporediesi
Biella, Italy

Email: robime@iol.it

Abstract: For many years accessible to the professional astronomer only, nowadays speckle interferometry benefits also the double star amateur community, thanks to the introduction of affordable CCD detectors and powerful computers. Following some seminal papers, a description is given of a method to estimate double star parameters from speckle images captured using a webcam. Results show that diffraction-limited measurements are indeed obtained even with a relatively small telescope under moderate seeing conditions. An application has been developed to perform all the required speckle analysis presented here.

Introduction

Seeing effects due to the atmospheric turbulence limit the resolution of ground-based telescopes. Even for small apertures (0.2—0.3 m), the seeing disk, under typical observing conditions, is larger than the theoretical Airy disk. Techniques based on speckle interferometry are then used to recover the original diffraction-limited intensity distribution. Previous publications, (Turner, *et al.* 1992; Turner, 2004), have already shown that amateur astronomers are now able to apply speckle interferometry to double star astrometry thanks to the availability of affordable high-quality CCD camera systems and powerful personal computers. Furthermore, the use of webcams is becoming more common among double star observers, (Hitchcock, 2007; Schlimmer, 2007). This paper further contributes to these recent developments by presenting a series of measurements made using a webcam and applying speckle interferometry. The accuracy of the method is checked against a selection of known double star positions, confirming that diffraction-limited measurements of close pairs can be obtained with a typical amateur telescope setup, even under moderate seeing conditions.

Observations

A 9.25" (0.233 m) Celestron, f/10, Schmidt-Cassegrain telescope is used with a 2.5X focal extender, resulting in a nominal focal length of 5.83 m. Image acquisition is performed with a Philips ToUcam Pro PCVC 840K color webcam, with a CCD chip made of an RGB matrix of 640x480 squared pixels (5.6 microns). Once fitted to the focal extender, the webcam is then connected to a laptop computer by a USB 1.1 port. This setup fulfills the Nyquist condition for digital image sampling, which requires that the pixel size should be smaller than half of the smallest details in the image plane we want to reconstruct. Based on speckle interferometry theory, the typical size of speckles is of the order of the Airy disk formed in the image plane by a point-like object. Thus in our case the pixel size should be at least smaller than half of the theoretical Airy disk. On the other side, pixels even smaller could result in a lower signal to noise ratio due to the reduction of light intensity per pixel. For a monochromatic source, given the objective diameter D, the source wavelength λ and the telescope focal length F, the Airy disk diameter in the focal plane is

$$d_{Airy} = \frac{1.22\lambda F}{D} \qquad (1)$$

assuming no central obstruction (Klein and Furtak, 1986).

For a non-monochromatic source, in case no narrow band filter is used, and a Schmidt-Cassegrain configuration with central obstruction, equation 1 still provides a reasonable estimate of the diameter of a speckle in the focal plane. In our case, using λ = 500 nm we get

$$d_{Airy} = \frac{1.22(5\times10^{-7}\,\text{m})(5.83\text{m})}{0.233\text{m}} = 15.26\ \mu\text{m}$$

which is greater than twice the pixel size, thus satisfying the Nyquist condition. Another very important requirement, which has to be satisfied during video capture, is to keep the single frame exposure time of the order of 20 ms or less, to actually *freeze* the speckle pattern. Since the software provided with the webcam does not allow setting the single frame exposure time explicitly, a combination of unofficial settings have been used instead (http://www.home.zonnet.nl/m.m.j.meijer/D_I_Y/webcam_shutter.htm). As a consequence of such a short exposure time, the application of speckle interferometry is limited to the brightest double stars only. In our case the magnitude limit is found to be around 7 when no filter is used. Finally, the frame rate has been set to 5 frames per second in order to limit data compression effects introduced by the USB 1.1 connection. This gives 300 color frames for a 1 minute video capture. The resulting AVI file is then converted to a sequence of black and white FIT format images, using IRIS (www.astrosurf.org/buil/us/iris/iris.htm).

Calibration

In a double star, the secondary component position relative to the primary component is initially found in terms of pixel coordinates, with the brighter component assumed to be at the origin (0,0). Calibration of the pixel scale and orientation is necessary in order to convert the measured secondary position to the separation and position angle (ρ,θ). Two methods have been considered here:

A) double stars with known separation and position angle are taken as references;

B) double stars images are recorded with the sidereal tracking stopped.

Both methods allow calibrating the image scale and, by changing the webcam orientation, to check that the CCD aspect ratio corresponds to the nominal values provided by the manufacturer. Method B was chosen here since it is rather straightforward and does not need a prior knowledge of other stars' separations and position angles. Further, it just requires us to stop the mount sidereal tracking on the same double star under measurement. Even so, method A has been also used in the early stages of this study with the very wide pair HIP100064-HIP100027 with no focal extender, to check the CCD aspect ratio by measuring their separation under different webcam orientations. No significant change in the pair separation under almost orthogonal directions was found, and the obtained mean value of 0.2239 arcsec/pixel agrees with the results later obtained with method B (see Table 1, setup (a)), once the effect of the focal extender is taken into account. Here follows a detailed description of method B used for this study.

Each video frame is processed to find the maximum intensity position, defined as the midpoint of the 5x5 pixel box with the maximum average intensity. The resulting sequence of (x_i^{max},y_i^{max}) data is finally linearly interpolated to get a (v_x,v_y) reference vector on the image plane for the East to West drift velocity, such that $x_i^{max} \cong x_o+v_x i$ and $y_i^{max} \cong y_o+v_y i$, where $i = 0..(N-1)$, N is the number of frames, and (x_o,y_o) is the initial position. Finally, the reference vector's module

$$v = \sqrt{{v_x}^2 + {v_y}^2}$$

which gives the average number of pixels per frame travelled by the moving star image when the tracking is stopped, is used in conjunction with the known star declination δ and video frame rate f_r (number of frames per second) to estimate the image scale (arcsec/pixel) as

$$i_s = \frac{15\cos\delta}{v f_r} \qquad (2)$$

The basic assumption for equation 2 is that no frame is lost during video acquisition, so that each frame is separated by an equal interval of time from the previous one. If some frames are dropped, as it may happen with a laptop computer when operating at low temperatures, eq. 2 cannot be used, since f_r is not constant. To avoid this problem the exact sequence of good and dropped frames must be known. Unfortunately IRIS (ver. 5.32) does not allow marking dropped frames, so no attempt has been done here to calculate the scale factor in these cases. Nevertheless, even if some frames are dropped, the image orientation can still be estimated by using the direction given by the reference vector (v_x,v_y). To conclude, the procedure used here for method B guarantees that for each video capture, the webcam orientation is measured,

Estimation of Double Star Parameters by Speckle Observations Using a Webcam

Setup	Mean (arcsec/pixel)	Std. Dev (arcsec/pixel)	Number of stars
(a)	0.2274	0.0018	9
(b)	0.2089	0.0025	5
(c)	0.2160	0.0045	10

Table 1: Image scale calibration factors obtained by capturing star images with the mount sidereal tracking stopped: (a) no additional focuser; (b) with additional focuser; (c) with additional focuser and a different adapter ring.

while an image scale factor is estimated only if no frame is dropped. In particular, each double star video capture is subsequently analyzed using its own specific reference vector for the orientation, and an image scale calculated as an average of all the measured scale factors available for that same optical setup. As regards the orientation, this is very important since the pointing accuracy of the setup used here, based on a commercial equatorial mount used at different locations, often requires removing the webcam to center the object using a lower focal length eyepiece, thus losing any previous calibration of the orientation. Table 1 summarizes the scale calibration results for three slightly different optical setups.

While this procedure worked quite well in almost all cases, a problem arose when a double star with two well separated components of very similar magnitude was considered, as in the case of STF 180AB. The switch, from one star to the other, of the estimated maximum intensity positions in the frame sequence, resulted in an unreliable estimate of the reference vector. Thus, a manual selection of each component position was required, before interpolation was carried out to calculate the reference vector. It is worth mentioning that recently, a similar automatic procedure to calibrate scale and orientation that avoids this problem has been presented in the JDSO by Ed Hitchcock (Hitchcock, 2007) and implemented in his software BinStar (`http://www.budgetastronomer.ca`). However, no attempt was made here to apply that improved procedure, since the only affected double star was STF 180AB.

Data Reduction

Different methods are used in speckle interferometry when it comes to data reduction. Some methods target a full image reconstruction based on the estimate of the Fourier power spectrum and bispectrum of the original intensity distribution (Glindemann, *et al.*, 1992; Horch, *et al.*, 1997; Fors, *et al.*, 2004), while others focus on the properties of the calculated two-dimentional autocorrelation function (Bagnuolo *et al.*, 1992). While the former approach could yield a reconstructed image, that is not only the relative position but also the relative intensity even for multiple stars systems, the latter is chosen here since it is easier to implement to estimate the parameters we are interested in, i.e. separation and position angle of double stars. The method used here is based on the original work of Bagnuolo *et al.*, in particular for the use of the *Directed Vector Autocorrelation (DVA)* algorithm to eliminate the 180° ambiguity in position angle measurement.

To summarize, let's start with the raw data, which in our case is stored in a color AVI file. Using IRIS, this AVI file is converted into a sequence of frames (640x480 pixels) stored in FIT format. Figure 1 shows a single frame of a video sequence of STF2583AB captured under moderate seeing.

There are actually four sequences of frames that can be created: red, green, blue and panchro (total intensity). The panchro sequence is a simple average, pixel by pixel, of the three color sequences. The analysis can be done for each sequence, independently. In principle, using a specific color sequence should yield more accurate results, compared to what could be

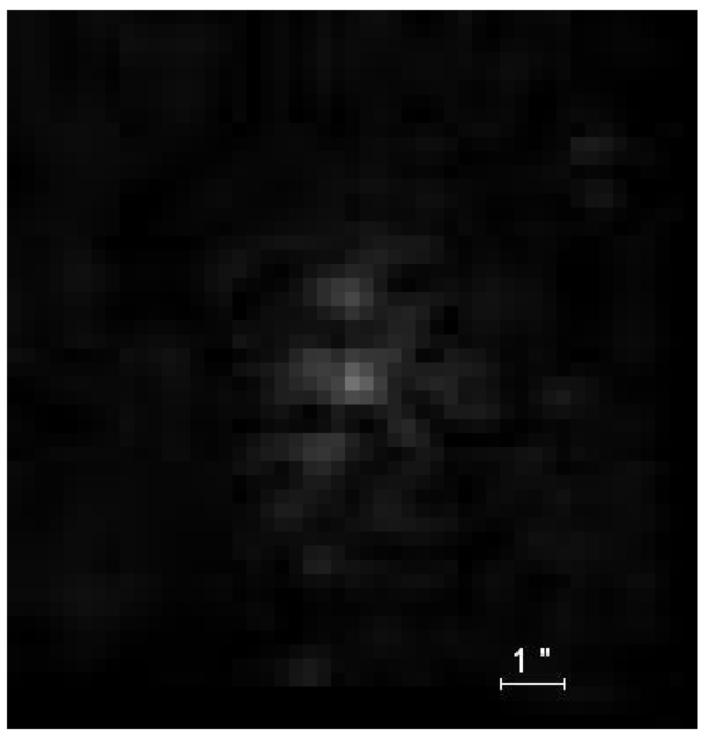

Figure 1: Example of speckle of STF 2583AB (0.216 arcsec/pixel).

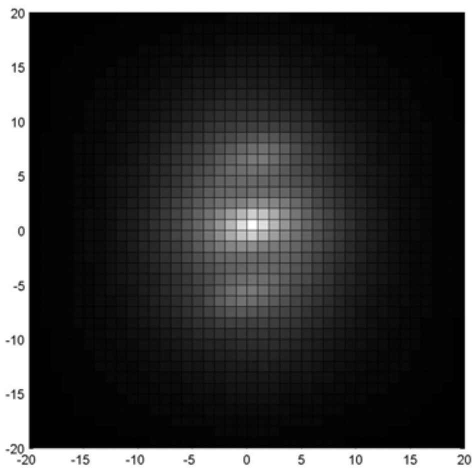

Figure 2: STF2583AB, autocorrelation matrix (0.216 arcsec/pixel)

obtained with the panchro sequence, since the dispersion effect induced by the atmosphere is reduced. Furthermore, in the case of the blue sequence, one could expect a greater theoretical resolution due to the shorter wavelength involved. On the other hand, the total intensity sequence results in a higher signal-to-noise ratio, particularly for low intensity doubles. Moreover, the Philips ToUcam Pro CCD chip uses a color filter mask where the red and blue pixels are double spaced, and the green pixels fill the remaining places (Bayer arrangement), thus reducing the actual resolution obtainable when using color sequences. From these considerations, it appears that using the panchro sequence is preferable in our case. So, in what follows, all the results will be reported for the panchro sequence only. It is also clear that a true monochromatic CCD based webcam with the same pixel size, possibly equipped with a color filter, would probably provide better results, as far as actual resolution and signal-to-noise ratio are concerned.

Preliminary statistics are calculated for each frame sequence, such as the average and the standard deviation of pixel intensities. These values are then used to set a minimum intensity threshold, below which a pixel intensity is set to zero. This in turn reduces the amount of data to be processed later, without a significant effect on the final results, as long as noise is lower than speckle intensity in the seeing disk. As a rule of thumb, a threshold given by the average intensity plus its standard deviation has been used here. The original intensity distribution $I^*_{i,j}$ is thus substituted by $I_{i,j} = I^*_{i,j} - T$ if $I^*_{i,j} \geq T$ or 0 if $I^*_{i,j} < T$, where i and j identify the pixel coordinates. The autocorrelation matrix $\boldsymbol{V}$ is then computed as

$$V_{i,j} = \sum_{s=1}^{N} \sum_{t=1}^{M} I_{s+i,t+j} I_{s,t} \qquad (3)$$

where N = 640 and M = 480 in our case, with appropriate padding to avoid effects at the edge. To speed up calculations, only the region surrounding the seeing disk is actually considered. By construction the autocorrelation matrix is symmetric, so only half of $\boldsymbol{V}$ is computed. The typical result depends on the relation between the actual double star separation ρ and the seeing disk width σ. If $\rho \gg \sigma$, three well separated peaks are found. The first one located at the origin (0,0) and the other two symmetrically displaced with respect to the first one. In this case i_{max} and j_{max} are easily found such that $V_{imax,jmax}$ is maximum (excluding the central peak region). In the other cases, when ρ is of the order of or even less than σ, the two secondary peaks appear superimposed on the primary peak, thus requiring an estimate of i_{max} and j_{max} that takes into account this effect. As described in (Bagnuolo *et al*, 1992), a boxcar subtraction routine can be applied, where a new matrix $\boldsymbol{V^*}$ is computed

$$V^*_{i,j} = V_{i,j} - \frac{1}{(2n+1)^2} \sum_{s=-n}^{s=n} \sum_{t=-n}^{t=n} V_{i+s,j+t} \qquad (4)$$

where in our case we have chosen n=2.

Again i_{max} and j_{max} such that $V^*_{imax,jmax}$ is maximum are searched for, excluding the central peak region, either automatically or by visual inspection of $\boldsymbol{V^*}$. In order to obtain a better estimate for the secondary star position, a simple weighted average of pixels positions around (i_{max}, j_{max}) is calculated, based on the values of $\boldsymbol{V^*}$ close to this maximum.

A 180° ambiguity still remains with respect to which one of the two secondary peaks actually represents the true secondary (i.e. fainter) component position. The DVA algorithm is used here to answer this question (Bagnuolo *et al.*, 1992). Briefly, the same procedure used to compute the autocorrelation matrix **V** is followed, the only difference being that each product $I_{s+i,t+j} I_{s,t}$ in eq. 3 is zeroed when $I_{s+i,t+j} > I_{s,t}$. The resulting DVA matrix is then used to check which

Estimation of Double Star Parameters by Speckle Observations Using a Webcam

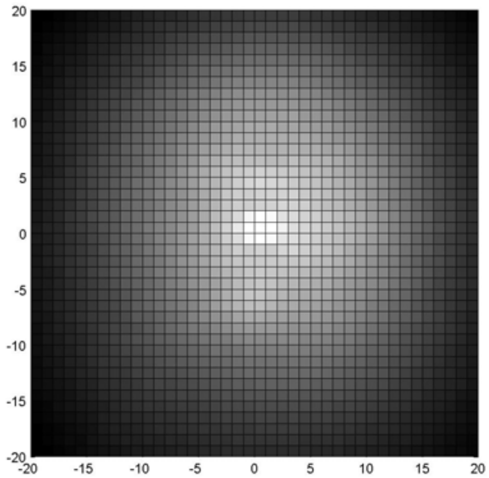

Figure 3: STF2583AB, directed vector autocorrelation matrix (0.216 arcsec/pixel)

secondary peak corresponds to the greater value in the DVA matrix, and the result taken as the best estimate for the secondary star position.

All the above procedures, except for the initial AVI conversion with IRIS, have been included in a software application called SIA, developed with a Borland Turbo C++ compiler on Windows XP. Import of the FIT format files makes use of the CFITSIO libraries (http://heasarc.gsfc.nasa.gov/docs/software/fitsio/). The program still needs some improvements in order to be more user friendly and portable, in particular for the formats supported, still limited to the 640 x 480 pixels case. It will be freely available as soon as these improvements will be completed.

Results

Observations were made in years 2006 and 2007 from three different locations in the Alps (Italy): Biella (45°33'N-8°2'E), Andrate (45°32'N-7°52'E) and Champorcher (45°37'N-7°44'E), under clear skies and generally moderate seeing conditions. Typical seeing disks were 2 to 3 arcsec wide, significantly greater than the theoretical resolution of the telescope used.

A series of known bright double stars were chosen to verify the procedure discussed above, with a particular focus on binary systems with separations just above the theoretical resolution. Each observation consisted of two video captures at least, one for the separation measurement and one for calibrating the webcam orientation, with the telescope tracking stopped. The results are given in Table 2.

For binaries where both components are of about the same intensity, the magnitude limit for detection is found to be around 7. Good results for close binaries are generally found, even if some non-zero autocorrelation in the CCD intensity noise can lead to a wrong detection of a secondary component position. Figure 2 shows an example of the computed autocorrelation matrix for STF 2583AB, while Figure 3 shows its directed vector autocorrelation matrix. In order to assess the accuracy of our setup, we compare the results reported in Table 2 with known positions derived from the Sixth Orbit Catalog or, when the ephemerides are not given, with the last available data in the WDS Catalog (http://ad.usno.navy.mil/wds/wds.html). Position angles and separations were calculated from the ephemerides by means of simple linear interpolation of the two closest calculated positions, given the time of observation. No attempt has been made to better refine the interpolation, since the uncertainties in our measurements are significantly greater than the uncertainties in the known positions. Errors are shown graphically in Figure 4. Overall the estimated standard deviation for both axes is 0.17 arcsec. For comparison purposes, the theoretical Airy disk for a telescope of the same aperture and no secondary obstruction is depicted. This comparison confirms that speckle interferometry provides diffraction-limited relative position measurements even when applied under moderate seeing conditions with a small telescope, at least for sufficiently bright double stars. A deeper analysis of Figure 4 suggests the existence of a correlation between the errors in the X and Y axes in our measurements, where the Y axes corresponds to the usual North direction used to report position angles. Despite some attempts to understand such a correlation, no clear explanation was found. More measurements are probably needed to further investigate this behavior.

In order to model the errors in (ρ,θ), the following assumptions were made: errors in the separation ρ are normally distributed with zero mean and standard deviation equal to σ_ρ with respect to known parameters. These errors derive from the autocorrelation procedure only, since the measured ρ does not depend on any step required to determine the webcam orientation. Errors in the position angle θ are also normally distributed with zero mean and a standard deviation due to a combination of both the uncertainty of the autocorrelation method and the uncertainty of the calibration of the webcam orientation. If we assume

(Continued on page 117)

RA+DEC	NAME	MAGS	DATE	ρ^m	θ^m	ρ^e	θ^e	$\Delta\rho$	$\Delta\theta$	N	NOTES
00063+5826	STF3062	6.42,7.32	2007.609	1.54	341.0	1.54	342.4	0.002	-1.40	1	3,4
			2007.839	1.27	353.3	1.54	342.8	-0.268	10.49	1	3,4
01535+1918	STF 180AB	4.52,4.58	2007.839	7.30	2.2	7.40	0.0	-0.100	2.20	1	3,5
02124+3018	STF 227	5.26,6.67	2007.839	3.69	67.6	4.00	69.0	-0.310	-1.40	1	3,5
02140+4729	STF 228	6.56,7.21	2007.034	0.72	289.7	0.90	289.2	-0.176	0.46	1	1,4,6
02592+2120	STF 333AB	5.17,5.57	2007.839	1.35	212.2	1.40	209.0	-0.050	3.20	1	3,5
06462+5927	STF 948AB	5.44,6.00	2006.979	1.94	62.2	1.86	69.9	0.077	-7.71	1	1,5,6
10163+1744	STT 215	7.25,7.46	2007.283	1.30	196.0	1.52	179.6	-0.221	16.36	1	1,4,6
			2007.376	1.33	182.7	1.52	179.6	-0.192	3.07	1	2,5
11182+3132	STF1523AB	4.33,4.80	2007.283	1.59	226.5	1.66	230.6	-0.069	-4.15	1	1,5
			2007.376	1.67	230.8	1.66	230.0	0.014	0.76	1	2,5
12417-0127	STF1670AB	3.48,3.53	2007.283	0.69	43.8	0.73	54.8	-0.041	-10.98	1	1,5,7
			2007.376	0.66	41.8	0.76	53.0	-0.095	-11.26	1	2,5,7
12533+2115	STF1687AB	5.15,7.08	2007.283	1.29	181.1	1.04	192.4	0.254	-11.31	1	1,5
			2007.376	1.03	191.4	1.04	192.5	-0.004	-1.14	1	2,5
14411+1344	STF1865AB	4.46,4.55	2007.283	0.66	304.1	0.60	296.0	0.058	8.10	1	1,5,6
			2007.376	0.79	292.5	0.60	295.9	0.194	-3.42	1	2,5
			2007.532	0.67	298.1	0.60	295.8	0.070	2.25	1	3,5
15038+4739	STF1909	5.20,6.10	2006.500	2.00	65.2	1.89	57.1	0.107	8.10	1	1,4
18101+1629	STF2289	6.65,7.21	2007.532	1.24	218.0	1.24	216.7	0.000	1.24	1	3,5
			2007.609	1.21	216.2	1.24	216.7	-0.030	-0.49	1	3,4
18359+1659	STT 358AB	6.94,7.08	2007.609	1.60	150.6	1.55	150.5	0.050	0.10	1	3,4
19487+1149	STF2583AB	6.34,6.75	2007.532	1.33	101.2	1.30	106.0	0.030	-4.80	2	3,5
			2007.609	1.37	103.3	1.30	106.0	0.074	-2.68	1	3,4
20474+3629	STT 413Aa-B	4.73,6.26	2006.500	1.02	351.3	0.90	3.7	0.118	-12.35	1	1,4
21021+5640	STF2751	6.23,6.89	2007.609	1.59	355.6	1.60	355.0	-0.007	0.60	2	3,4
			2007.839	1.25	12.7	1.60	355.0	-0.347	17.70	1	3,4
22288-0001	STF2909	4.34,4.39	2006.639	1.59	176.3	2.13	177.8	-0.545	-1.51	1	1,5
23595+3343	STF3050AB	6.46,6.72	2007.839	2.28	331.9	2.09	334.3	0.192	-2.37	1	3,4

Table 2: Double star speckle measures. All measures taken by speckle interferometry using a 9.25 inch (0.233 m) f/10 Celestron SCT with a Televue 2.5X focal extender and a Philips ToUcam Pro PCVC 840K webcam (5.6 micron pixels). (ρ^m,θ^m) are measured parameters, (ρ^e,θ^e) are known parameters and ($\Delta\rho$,$\Delta\theta$) are O-C values

Notes:

1. 0.2274 +/- 0.0018 arcsec/pixel
2. 0.2089 +/- 0.0025 arcsec/pixel
3. 0.2160 +/- 0.0045 arcsec/pixel
4. 1/50 shutter speed, 5 frames per second, 40 ms exposure time, 300 frames
5. 1/100 shutter speed, 5 frames per second, 20 ms exposure time, 300 frames
6. Secondary peak of the autocorrelation matrix manually selected due to significant residual noise autocorrelation.
7. 180°-reversed after comparison with known position angle.

Estimation of Double Star Parameters by Speckle Observations Using a Webcam

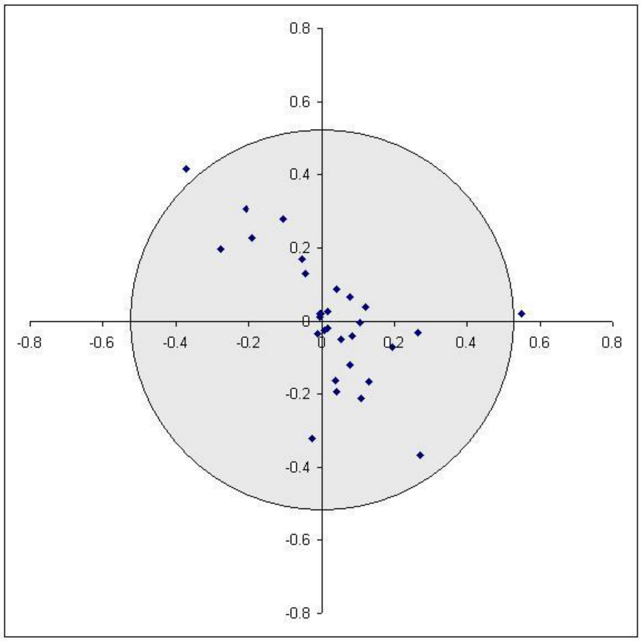

Figure 4: Estimated errors (arcsec) of double star measures reported in table 2. For comparison purposes, the circle represents the theoretical Airy disk for a 23.3 cm aperture telescope with no secondary obstruction and a 500 nm monochromatic source.

(Continued from page 115)

that these two sources of errors are not correlated, as it should be since the two procedures involved are independent, we can model the total error for θ, given the separation ρ, as

$$\sigma_\theta(\rho) = \sqrt{\left(\frac{\sigma_\rho}{\rho}\right)^2 + \sigma_{or}^2} \qquad (5)$$

where σ_ρ / ρ is the error in θ due to the autorrelation method only, once the transformation from Cartesian coordinates to polar coordinates is taken into account, and σ_{or} is the error due to the method used to calibrate the orientation. An estimate for σ_ρ is easily found to be 0.15 arcsec based on the data reported in Table 2. To estimate the value of σ_{or} a Bayesian approach is followed to calculate its posterior probability distribution function $p(\sigma_{or})$, which is proportional to the likelihood of σ_{or} given our data for the measured position angles θ^n versus the known parameters θ^e and ρ^e

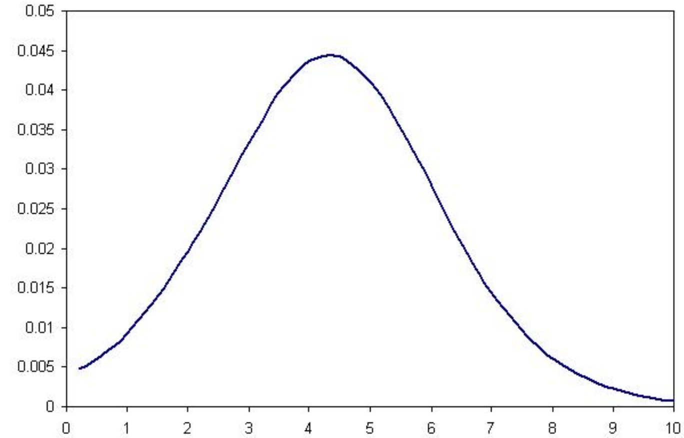

Figure 5: Probability distribution function for the calibration error σ_{or} (degrees) of the webcam orientation.

$$p(\sigma_{or}) \propto \prod_{k=1}^{N} \frac{1}{\sqrt{2\pi}\sigma_\theta} e^{-\frac{(\theta_k^m - \theta_k^e)^2}{2\sigma_\theta^2}} \qquad (6)$$

If we consider the natural logarithm of $p(\sigma_{or})$, by substituting eq. 5 in eq. 6 we get:

$$log\, p(\sigma_{or}) = -\frac{1}{2}\sum_{k=1}^{N} \frac{(\theta_k^m - \theta_k^e)^2}{\left(\frac{\sigma_\rho}{\rho_k^e}\right)^2 + \sigma_{or}^2} - \frac{1}{2}\sum_{k=1}^{N} \log\left[\left(\frac{\sigma_\rho}{\rho_k^e}\right)^2 + \sigma_{or}^2\right] + c \qquad (7)$$

where c does not depend on σ_{or}, if we assume no prior knowledge except that $\sigma_{or} \geq 0$, and the sum runs on all double stars in Table 2. A plot of $p(\sigma_{or})$ after normalization is shown in Figure 5. The best estimate for σ_{or} can be found by maximizing $p(\sigma_{or})$, i.e. by taking the derivative of eq. 7 versus σ_{or} and finding its zero, as given by eq. 8 for $\sigma_{or} > 0$

Estimation of Double Star Parameters by Speckle Observations Using a Webcam

Magnitude Limit	σ_ρ(arcsec)	σ_{or}(rad)
≈ 7	0.15	0.075

Table 3: Magnitude limit and best error estimate for double star parameters obtained by speckle measurements.

$$\sum_{k=1}^{N} \frac{(\theta_k^m - \theta_k^e)^2 - \left(\frac{\sigma_\rho}{\rho_k^e}\right)^2 - \sigma_{or}^2}{\left[\left(\frac{\sigma_\rho}{\rho_k^e}\right)^2 + \sigma_{or}^2\right]^2} = 0 \qquad (8)$$

The best estimate for σ_{or} was found to be 0.075 rad (4.3°). These results are summarized in Table 3, where magnitude limit, uncertainty in separation and position angle are given, based on results reported in Table 2 and taking into account our model for the total error in position angle based on eq. 5.

As an example, if we consider STF333AB, the best estimate for the uncertainty in θ based on eq. 5 and data in table 2 is

$$\sigma_\theta = \frac{180}{\pi}\sqrt{\left(\frac{0.15}{1.35}\right)^2 + 0.075^2} = 7.68 \qquad (9)$$

which gives $\rho = 1.35 \pm 0.15$ and $\theta = 212.2 \pm 7.68$.

Conclusions

Seeing effects due to the atmospheric turbulence and tracking errors of common commercial mounts used by amateurs are the main sources of image blurring and loss of resolution. The very short exposure times used in speckle interferometry are intended to recover the original intensity distribution or some related data such as position angle and separation of a double star. The main advantage of the technique is to allow for the relative position of a double star to be measured with a limiting resolution comparable to the diffraction limit of the telescope, provided the CCD pixel scale and orientation are properly calibrated. The main disadvantage remains the rather low sensitivity, both in the limiting magnitude and on the maximum difference between the two components' magnitude.

Overall, the reported measurements confirm the potential benefit of speckle interferometry even for amateur astronomers using a small telescope. A programm called SIA has been developed to implement the analysis presented here, and work is in progress to make it more user friendly and freely available.

Acknowledgements

The author wishes to thank Carlo Perotti for useful discussions and support during observations. This research has made use of the CFITSIO software library maintained by Dr. William D. Pence, IRIS, Cartes du Ciel and the Washington Double Star Catalog maintained by the U. S. Naval Observatory.

References

Bagnuolo, William G. Jr., Mason, B.D., Barry, D.J., Hartkopf, W.I., and McAlister, H.A., 1992, *Astron. J.*, **103**(4), 1399-1407.

Fors, Octavi, Horch, E.P., and Nunez, J., 2004, *Astron. Astrophys.*, **420**, 397-404.

Glindemann, A., Lane, R.G., and Dainty, J.C., 1992, *J. Opt. Soc. Am. A*, **9**(4), 543-548.

Hitchcock, Ed, 2007, *Journal of Double Star Observations*, **3**(1), 17-20.

Horch, Elliott P., Zoran, N., and Slawson, R.W., 1997, *Astron J.*, **114**(5), 2117-2127.

Klein, M.V., and Furtak, T.E., 1986, *Optics*, pg. 363, Wiley & Sons.

Schlimmer, Joerg, 2007, *Journal of Double Star Observations*, **3**(3), 131-134.

Turner, Nils H., Barry, D.J., and McAlister, H.A., 1992, *Astro. Soc. Pacific Conf. Series*, **32**, 577-579.

Speckle Interferometry for the Amateur, Turner, N., in *Observing and Measuring Double Stars*, Ed. Bob Argyle, Chapter **17**, Springer-Verlag, London 2004.

After graduating in physics, the author worked for some years in the field of vacuum science and gas-surface interactions and then moved to the financial industry to become a trader on equity derivatives. He tells us that only recently his early interest in astronomy returned, and now "double star imaging gives me the opportunity to turn a little to science again."